Image Compression With Haar Wavelets

Alex Beeny

April 2, 2021

1 Haar Wavelet

Wavelets are described by a mother function $\psi(t)$ accompanied by a father (or scaling) function $\phi(t)$. For the Haar wavelet, these functions are defined as

$$\psi(t) = \begin{cases} 1\,, & 0 \le t < 1/2, \\ -1\,, & 1/2 \le t \le 1, \\ 0\,, & \text{otherwise.} \end{cases} \quad \text{and} \quad \phi(t) = \begin{cases} 1\,, & 0 \le t \le 1, \\ 0\,, & \text{otherwise,} \end{cases} \tag{1}$$

For $\psi(t)$ to be a wavelet, we require that it integrates to zero on its domain.

1.1 Child Wavelets

The Haar wavelet's support is the unit interval $[0, 1]$. We can contract the mother function to get a wavelet half the size on the interval $[0, 1/2]$, namely $\psi(2t)$. Also, translating to fit the interval $[1/2, 1]$, we get $\psi(2t - 1)$. See Figure 1. Since these smaller wavelets are derived from the mother, we call them daughter wavelets distinguishing them by parameters in subscripts, $\psi_{1,0}(t) = \psi(2^1 t - 0) = \psi(2t)$ and $\psi_{1,1}(t) = \psi(2^1 t - 1) = \psi(2t - 1)$. Likewise, son wavelets are derived from the father function.

2 Wavelet Basis

Our primary goal is to approximate a signal $f(t)$ using wavelets. We will see that we are limited to signals with finite energy, that is $f(t)$ must be in the Hilbert space $L^2(\mathbb{R}) = \left\{ f \;\middle|\; f : \mathbb{R} \to \mathbb{R}, \int_{-\infty}^{\infty} f^2 < \infty \right\}$, the set of all square integrable functions.

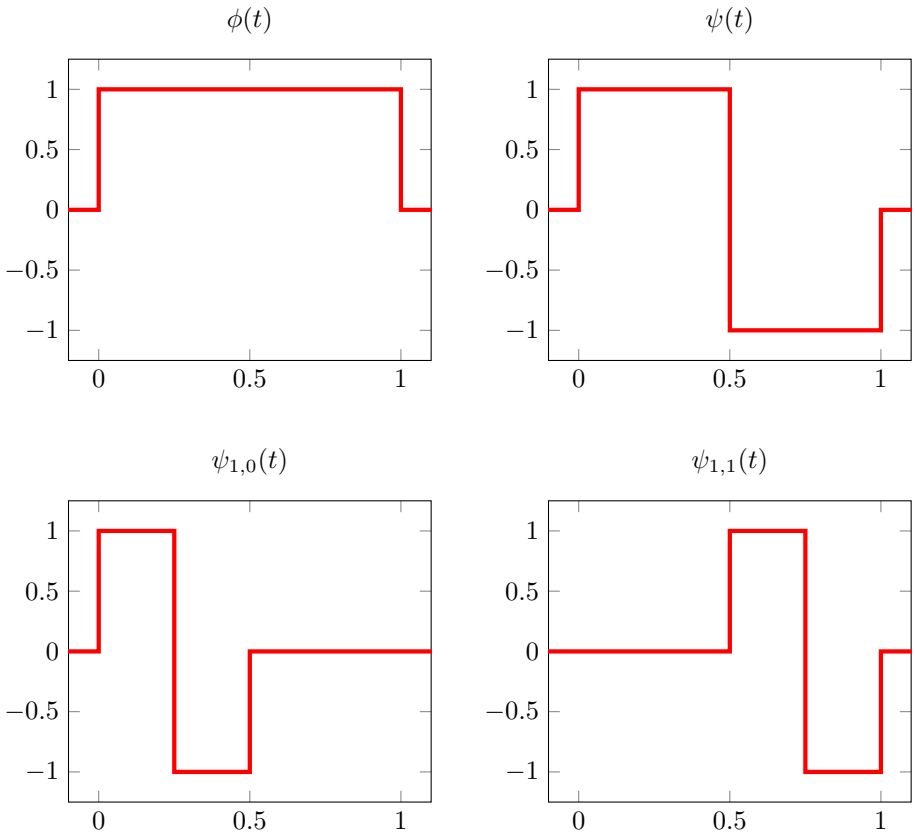

Figure 1: First generation of Haar wavelet functions.

2.1 Multiresolution Analysis

A nice feature of many wavelets, including the Haar, is the *multiresolution analysis* (MRA) property, which provides a method to improve computational efficiency. Consider the function space $V_j = \text{span}\,\{\phi(2^j t - k) \mid k \in \mathbb{Z}\}$ describing the subspace of $L^2(\mathbb{R})$ generated by 2^j resolution father functions. A function $f \in L^2(\mathbb{R})$ can be approximated by the projection of f onto V_j, that is

$$f_j(t) = \sum_{k\in\mathbb{Z}} h_k \phi(2^j t - k) \in V_j, \quad \text{where} \quad h_k = \langle f, \sqrt{2}\phi(2^j t - k)\rangle. \tag{2}$$

Notice that $\phi(t)$ lives in the reference space V_0. Then $\phi(t)$ can be represented as a linear combination of functions in V_1 and we have $V_0 \subset V_1$. In general,

we have a sequence of nested subspaces such that

$$\cdots \subset V_{-1} \subset V_0 \subset V_1 \subset \cdots \subset L^2(\mathbb{R}), \tag{3}$$

forming a multiresolution analysis. In the case of the Haar wavelet, the MRA allows us to construct the mother function from our choice of the father function $\phi(t) = 1$ on the unit interval and zero otherwise. Then W_j is generated by $\{\psi(2^j t - k) \mid k \in \mathbb{Z}\}$ such that $V_{j+1} = V_j \oplus W_j$. In other words, W_j contains the information that is lost when a function is approximated at a lower resolution. For $f_j \in V_j$ and $w_j \in W_j$, the n-level decomposition of a function $f_n \in V_n$ is given by

$$f_n = f_{n-1} + w_{n-1} = f_{n-2} + w_{n-2} + w_{n-1} = \cdots = f_0 + w_0 + w_1 + \cdots + w_{n-1},$$

where f_j and w_j are called the *average details* and *difference details*, respectively, at the j-th level.

2.2 Orthogonality of the Haar Wavelet

In the previous section, we constructed a spanning set using $\phi(t)$ to approximate a function $f(t) \in L^2(\mathbb{R})$. Using the relationship between the Haar wavelet functions, we see that $\psi(t) = \phi(2t) - \phi(2t-1)$. Then it follows that we can construct a spanning set using $\psi(t)$ such that

$$f(t) = \sum_{k \in \mathbb{Z}} g_k \psi(2^j t - k), \tag{4}$$

where g_k are some scaling coefficients. Notice that as j increases, the spaces spanned by these sets approach $L^2(\mathbb{R})$.

By orthogonality, we can show that these spanning sets are linearly independent and, therefore, form an orthogonal basis. First, we see that the functions in V_j are disjoint and the functions in W_j are disjoint, so the pairwise inner products in each space are always zero. Also, if $\phi_{j,k} \in V_j$ is translated by k and $\psi_{j,k'} \in W_j$ is translated by k' with $k \neq k'$, then $\phi_{j,k}$ and $\psi_{j,k'}$ are disjoint with an inner product of zero. So, suppose $\phi_{j,k}$ and $\psi_{j,k}$ have the same support, for example, consider $\phi = \phi_{0,0}$ and $\psi = \psi_{0,0}$ on the unit interval. Then

$$\langle \phi, \psi \rangle = \int_{-\infty}^{\infty} \phi(t)\overline{\psi(t)}\,\mathrm{d}t = \int_{-\infty}^{\infty} \phi(t)\psi(t)\,\mathrm{d}t = \int_0^{1/2} 1\,\mathrm{d}t - \int_{1/2}^{1} 1\,\mathrm{d}t = 0.$$

Other cases are similar, so we can conclude $\langle \phi_{j,k}, \psi_{j,k} \rangle = 0$ for all $j, k \in \mathbb{Z}$. Hence, the Haar wavelet functions ϕ and ψ form an orthogonal basis under $t \mapsto (2^j t - k)$ mappings.

2.3 Vector Representation

For computations, it is convenient to represent wavelets as vectors. For example, we can define the first generation of wavelet vectors as

$$\begin{aligned} \phi &\equiv (1,1,1,1), & \psi &\equiv (1,1,-1,-1), \\ \psi_{1,0} &\equiv (1,-1,0,0), & \psi_{1,1} &\equiv (0,0,1,-1), \end{aligned}$$

which span $\mathbb{R}^4$. Further, we can demonstrate that these vectors are mutually orthogonal by computing each of the inner products

$$\begin{aligned} \langle \psi, \phi \rangle &= (1,1,-1,-1)(1,1,1,1)^T = 1+1-1-1 = 0, \\ \langle \psi_{1,0}, \phi \rangle &= (1,-1,0,0)(1,1,1,1)^T = 1-1+0+0 = 0, \\ \langle \psi_{1,1}, \phi \rangle &= (0,0,1,-1)(1,1,1,1)^T = 0+0+1-1 = 0, \\ \langle \psi_{1,0}, \psi \rangle &= (1,-1,0,0)(1,1,-1,-1)^T = 1-1+0+0 = 0, \\ \langle \psi_{1,1}, \psi \rangle &= (0,0,1,-1)(1,1,-1,-1)^T = 0+0-1+1 = 0, \\ \langle \psi_{1,0}, \psi_{1,1} \rangle &= (1,-1,0,0)(0,0,1,-1)^T = 0+0+0+0 = 0. \end{aligned}$$

As in the continuous case, we see that the wavelet vectors form an orthogonal basis. It will be especially useful to normalize these vectors so that the total energy of a function is not changed. Thus, when we divide by the norms $\|\phi\| = 2$, $\|\psi\| = 2$, $\|\psi_{1,0}\| = \sqrt{2}$, and $\|\psi_{1,1}\| = \sqrt{2}$, we obtain an orthonormal wavelet basis.

3 Decomposition and Reconstruction

In general, a wavelet decomposition is obtained using wavelet transforms. A series of inner products are computed using the signal function and wavelet for each level of the decomposition. Due to the MRA property, these computations can be performed for the Haar wavelet using a simple algorithm. Moreover, since the difference details contain the exact error for an approximation, the original signal can be perfectly reconstructed.

The Haar wavelet transform $\mathcal{H}_1$ decomposes a signal $\mathbf{f}$ in $\mathbb{R}^n$ into the first average detail $\mathbf{a}^1$ and first difference detail $\mathbf{d}^1$, denoted

$$\mathbf{f} \xrightarrow{\mathcal{H}_1} (\mathbf{a}^1 \mid \mathbf{d}^1). \tag{5}$$

3.1 Decomposition Algorithm

Let $\mathbf{f} = (f_1, f_2, \ldots, f_n)$ be a signal with n even[1]. The average of the first two entries in $\mathbf{f}$ is computed by

$$a_1^1 = \frac{1}{\sqrt{2}}(1, 1, 0, 0, \ldots, 0)\mathbf{f}^T = \frac{f_1 + f_2}{\sqrt{2}}.$$

In general, the average detail of the mth pair of entries in $\mathbf{f}$ is found using the formula

$$a_m = \frac{f_{2m-1} + f_{2m}}{\sqrt{2}}, \tag{6}$$

for $m = 1, 2, \ldots, n/2$. Similarly, the difference detail is computed by

$$d_m = \frac{f_{2m-1} - f_{2m}}{\sqrt{2}}. \tag{7}$$

Then we obtain $\mathbf{a}^1 = (a_1^1, a_2^1, \ldots, a_{n/2}^1)$ and $\mathbf{d}^1 = (d_1^1, d_2^1, \ldots, d_{n/2}^1)$.

Example 3.1. Let $\mathbf{f} = (-1, 1, 9, 4, 7, 6, -4, 10)$. We find the first average details using Equation (6)

$$a_1^1 = \frac{-1+1}{\sqrt{2}} = \frac{0}{\sqrt{2}}, \qquad a_2^1 = \frac{9+4}{\sqrt{2}} = \frac{13}{\sqrt{2}},$$
$$a_3^1 = \frac{7+6}{\sqrt{2}} = \frac{13}{\sqrt{2}}, \qquad a_4^1 = \frac{-4+10}{\sqrt{2}} = \frac{6}{\sqrt{2}},$$

and the first difference details using Equation (7)

$$d_1^1 = \frac{-1-1}{\sqrt{2}} = \frac{-2}{\sqrt{2}}, \qquad d_2^1 = \frac{9-4}{\sqrt{2}} = \frac{5}{\sqrt{2}},$$
$$d_3^1 = \frac{7-6}{\sqrt{2}} = \frac{1}{\sqrt{2}}, \qquad d_4^1 = \frac{-4-10}{\sqrt{2}} = \frac{-14}{\sqrt{2}}.$$

Then we have

$$\mathbf{a}^1 = \frac{1}{\sqrt{2}}(0, 13, 13, 6), \qquad \mathbf{d}^1 = \frac{1}{\sqrt{2}}(-2, 5, 1, -14).$$

[1]If this is not the case, then a zero entry is appended to the signal.

3.2 Multi-Level Decomposition

After obtaining a decomposed signal $(\mathbf{a}^1 \mid \mathbf{d}^1)$, we can continue breaking the average detail into smaller components. Using the second level Haar wavelet transform, we have

$$\mathbf{f} \xrightarrow{\mathcal{H}_1} (\mathbf{a}^1 \mid \mathbf{d}^1) \xrightarrow{\mathcal{H}_2} (\mathbf{a}^2 \mid \mathbf{d}^2 \mid \mathbf{d}^1).$$

The justification for this is due to the MRA property of the Haar wavelet. Moreover, this method is known as a *cascade algorithm* and it allows us to compute the wavelet transform efficiently.

Example 3.2. Continuing Example 3.1, we apply the decomposition formulas to the first average detail $\mathbf{a}^1$. Thus

$$\begin{aligned} a_1^2 &= \frac{0 + \frac{13}{\sqrt{2}}}{\sqrt{2}} = \frac{13}{2}, \quad & a_2^2 &= \frac{\frac{13}{\sqrt{2}} + \frac{6}{\sqrt{2}}}{\sqrt{2}} = \frac{19}{2} \quad & \Longrightarrow \quad \mathbf{a}^2 &= \frac{1}{2}(13, 19); \\ d_1^2 &= \frac{0 - \frac{13}{\sqrt{2}}}{\sqrt{2}} = \frac{-13}{2}, \quad & d_2^2 &= \frac{\frac{13}{\sqrt{2}} - \frac{6}{\sqrt{2}}}{\sqrt{2}} = \frac{7}{2} \quad & \Longrightarrow \quad \mathbf{d}^2 &= \frac{1}{2}(-13, 7). \end{aligned}$$

3.3 Matrix Representation of the Decomposition

Instead of iteratively applying Equations (6) and (7), we can combine the steps using matrices. For a given signal $\mathbf{f}$ of length n, we define

$$H = \frac{1}{\sqrt{2}} \begin{pmatrix} 1 & 1 & 0 & 0 & \cdots & 0 \\ 0 & 0 & 1 & 1 & \cdots & 0 \\ \vdots & \vdots & & \ddots & \ddots & \vdots \\ 0 & 0 & \cdots & & 1 & 1 \end{pmatrix}, \quad G = \frac{1}{\sqrt{2}} \begin{pmatrix} 1 & -1 & 0 & 0 & \cdots & 0 \\ 0 & 0 & 1 & -1 & \cdots & 0 \\ \vdots & \vdots & & \ddots & \ddots & \vdots \\ 0 & 0 & \cdots & & 1 & -1 \end{pmatrix}, \tag{8}$$

where H and G each have $n/2$ rows and n columns. Now, we can write the Haar wavelet decomposition as $\mathbf{a}^1 = H\mathbf{f}$ and $\mathbf{d}^1 = G\mathbf{f}$ to get the matrix equation

$$\begin{pmatrix} \mathbf{a}^1 \\ \mathbf{d}^1 \end{pmatrix} = \begin{pmatrix} H\mathbf{f} \\ G\mathbf{f} \end{pmatrix} = \begin{pmatrix} H \\ G \end{pmatrix} \mathbf{f}. \tag{9}$$

3.4 Reconstruction

Since H and G were constructed from an orthonormal Haar wavelet basis, the matrix $\binom{H}{G}$ is orthonormal as well. Then left-hand multiplication by $\binom{H}{G}^T$ will allow us to solve for $\mathbf{f}$, and we get

$$\mathbf{f} = \begin{pmatrix} H \\ G \end{pmatrix}^T \begin{pmatrix} \mathbf{a}^1 \\ \mathbf{d}^1 \end{pmatrix} = (H^T \mid G^T) \begin{pmatrix} \mathbf{a}^1 \\ \mathbf{d}^1 \end{pmatrix} = H^T\mathbf{a}^1 + G^T\mathbf{d}^1. \tag{10}$$

Therefore, we say that the signal is *reconstructed* by the inverse Haar wavelet transform

$$(\mathbf{a}^1 \mid \mathbf{d}^1) \xrightarrow{\mathcal{H}_1^{-1}} \mathbf{f}. \tag{11}$$

Example 3.3. Let $\mathbf{a}^1$ and $\mathbf{d}^1$ be given from Example 3.1 as

$$\mathbf{a}^1 = \left(0, \frac{13}{\sqrt{2}}, \frac{13}{\sqrt{2}}, \frac{6}{\sqrt{2}}\right), \qquad \mathbf{d}^1 = \left(\frac{-2}{\sqrt{2}}, \frac{5}{\sqrt{2}}, \frac{1}{\sqrt{2}}, \frac{-14}{\sqrt{2}}\right).$$

To reconstruct $\mathbf{f}$ we compute $H^T\mathbf{a}^1$ and $G^T\mathbf{d}^1$.

$$H^T\mathbf{a}^1 = \frac{1}{\sqrt{2}} \begin{pmatrix} 1 & 0 & 0 & 0 \\ 1 & 0 & 0 & 0 \\ 0 & 1 & 0 & 0 \\ 0 & 1 & 0 & 0 \\ 0 & 0 & 1 & 0 \\ 0 & 0 & 1 & 0 \\ 0 & 0 & 0 & 1 \\ 0 & 0 & 0 & 1 \end{pmatrix} \cdot \frac{1}{\sqrt{2}} \begin{pmatrix} 0 \\ 13 \\ 13 \\ 6 \end{pmatrix} = \frac{1}{2} \begin{pmatrix} 0 \\ 0 \\ 13 \\ 13 \\ 13 \\ 13 \\ 6 \\ 6 \end{pmatrix}$$

$$G^T\mathbf{d}^1 = \frac{1}{\sqrt{2}} \begin{pmatrix} 1 & 0 & 0 & 0 \\ -1 & 0 & 0 & 0 \\ 0 & 1 & 0 & 0 \\ 0 & -1 & 0 & 0 \\ 0 & 0 & 1 & 0 \\ 0 & 0 & -1 & 0 \\ 0 & 0 & 0 & 1 \\ 0 & 0 & 0 & -1 \end{pmatrix} \cdot \frac{1}{\sqrt{2}} \begin{pmatrix} -2 \\ 5 \\ 1 \\ -14 \end{pmatrix} = \frac{1}{2} \begin{pmatrix} -2 \\ 2 \\ 5 \\ -5 \\ 1 \\ -1 \\ -14 \\ 14 \end{pmatrix}$$

Then we have

$$\mathbf{f} = H^T\mathbf{a}^1 + G^T\mathbf{d}^1 = \frac{1}{2}\begin{pmatrix}0\\0\\13\\13\\13\\13\\6\\6\end{pmatrix} + \frac{1}{2}\begin{pmatrix}-2\\2\\5\\-5\\1\\-1\\-14\\14\end{pmatrix} = \frac{1}{2}\begin{pmatrix}-2\\2\\18\\8\\14\\12\\-8\\20\end{pmatrix} = \begin{pmatrix}-1\\1\\9\\4\\7\\6\\-4\\10\end{pmatrix}.$$

3.5 Two-Dimensional Haar Wavelet Transform

The idea of signal decomposition using the Haar wavelet can be extended so that we can transform a matrix $\mathbf{f}$ into first-level details. Then we have

$$\mathbf{f} \xrightarrow{\mathcal{H}_1} \left(\begin{array}{c|c}\mathbf{a}^1 & \mathbf{h}^1\\ \hline \mathbf{v}^1 & \mathbf{d}^1\end{array}\right), \tag{12}$$

where $\mathbf{h}^1$ is the horizontal difference detail, $\mathbf{v}^1$ is the vertical difference detail, and $\mathbf{d}^1$ is the diagonal difference detail. If $\mathbf{f}$ is an $m \times n$ signal matrix, for m and n even[2], then the first-level details can be computed using a similar matrix algorithm to obtain

$$\mathbf{a}^1 = H\mathbf{f}H^T, \qquad \mathbf{h}^1 = H\mathbf{f}G^T, \qquad \mathbf{v}^1 = G\mathbf{f}H^T, \qquad \mathbf{d}^1 = G\mathbf{f}G^T, \tag{13}$$

where H and G on the left are sized $m/2 \times m$ and H^T and G^T on the right are sized $n \times n/2$ so that multiplication is defined.

Example 3.4. Consider the 4×4 grayscale image with intensity values ranging from 0 (black) to 255 (white) represented as a matrix $\mathbf{f}$.

$$\mathbf{f} = \begin{pmatrix}67 & 148 & 159 & 19\\ 37 & 140 & 89 & 61\\ 35 & 37 & 131 & 31\\ 22 & 218 & 102 & 47\end{pmatrix} \quad \longleftrightarrow \quad$$

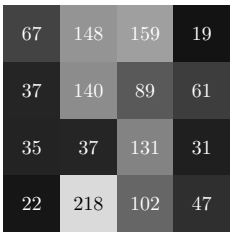

[2]If this is not the case, then add a row and/or column of zeros to $\mathbf{f}$ to make the dimensions even.

The average detail $\mathbf{a}^1$ is found in two steps. First we compute detail from the columns by the left-hand multiplication

$$\begin{aligned} H\mathbf{f} &= \frac{1}{\sqrt{2}}\begin{pmatrix}1 & 1 & 0 & 0\\ 0 & 0 & 1 & 1\end{pmatrix}\begin{pmatrix}67 & 148 & 159 & 19\\ 37 & 140 & 89 & 61\\ 35 & 37 & 131 & 31\\ 22 & 218 & 102 & 47\end{pmatrix} \\ &= \frac{1}{\sqrt{2}}\begin{pmatrix}67+37 & 148+140 & 159+89 & 19+61\\ 35+22 & 37+218 & 131+102 & 31+47\end{pmatrix} \\ &= \frac{1}{\sqrt{2}}\begin{pmatrix}104 & 288 & 248 & 80\\ 57 & 255 & 233 & 78\end{pmatrix} \end{aligned}$$

Then we find $\mathbf{a}^1$ by the right-hand multiplication

$$\begin{aligned} \mathbf{a}^1 = (H\mathbf{f})H^T &= \frac{1}{\sqrt{2}}\begin{pmatrix}104 & 288 & 248 & 80\\ 57 & 255 & 233 & 78\end{pmatrix}\cdot\frac{1}{\sqrt{2}}\begin{pmatrix}1 & 0\\ 1 & 0\\ 0 & 1\\ 0 & 1\end{pmatrix} \\ &= \frac{1}{2}\begin{pmatrix}104+288 & 248+80\\ 57+255 & 233+78\end{pmatrix} \\ &= \frac{1}{2}\begin{pmatrix}392 & 328\\ 312 & 311\end{pmatrix} \end{aligned}$$

Similarly, we can find $\mathbf{h}^1$, $\mathbf{v}^1$, and $\mathbf{d}^1$ to get

$$\mathbf{a}^1 = \frac{1}{2}\begin{pmatrix}392 & 328\\ 312 & 311\end{pmatrix}, \qquad \mathbf{h}^1 = H\mathbf{f}G^T = \frac{1}{2}\begin{pmatrix}-184 & 168\\ -198 & 155\end{pmatrix},$$

$$\mathbf{v}^1 = G\mathbf{f}H^T = \frac{1}{2}\begin{pmatrix}38 & 28\\ -168 & 13\end{pmatrix}, \qquad \mathbf{d}^1 = G\mathbf{f}G^T = \frac{1}{2}\begin{pmatrix}22 & 112\\ 194 & 45\end{pmatrix}.$$

Finally, we write the decomposition as

$$\frac{1}{2}\left(\begin{array}{rr|rr} 392 & 328 & -184 & 168\\ 312 & 311 & -198 & 155\\ \hline 38 & 28 & 22 & 112\\ -168 & 13 & 194 & 45\end{array}\right) = \left(\begin{array}{rr|rr} 196 & 164 & -92 & 84\\ 156 & 155.5 & -99 & 77.5\\ \hline 19 & 14 & 11 & 56\\ -84 & 6.5 & 97 & 22.5\end{array}\right).$$

Reconstruction is obtained by the two-dimensional inverse Haar transform. Since $\binom{H}{G}$ and $\binom{H}{G}^T$ are orthonormal matrices, we have

$$\binom{H}{G}\mathbf{f}(H^T \mid G^T) = \binom{Hf}{Gf}(H^T \mid G^T) = \left(\begin{array}{c|c} HfH^T & HFG^T\\ \hline GfH^T & GfG^T\end{array}\right) = \left(\begin{array}{c|c} \mathbf{a}^1 & \mathbf{h}^1\\ \hline \mathbf{v}^1 & \mathbf{d}^1\end{array}\right).$$

Then

$$\begin{aligned}
\mathbf{f} &= \begin{pmatrix} H \\ G \end{pmatrix}^T \left(\begin{array}{c|c} \mathbf{a}^1 & \mathbf{h}^1 \\ \hline \mathbf{v}^1 & \mathbf{d}^1 \end{array}\right) (H^T \mid G^T)^T \\
&= (H^T \mid G^T) \left(\begin{array}{c|c} \mathbf{a}^1 & \mathbf{h}^1 \\ \hline \mathbf{v}^1 & \mathbf{d}^1 \end{array}\right) \begin{pmatrix} H \\ G \end{pmatrix} \\
&= (H^T\mathbf{a}^1 + G^T\mathbf{v}^1 \mid H^T\mathbf{h}^1 + G^T\mathbf{d}^1) \begin{pmatrix} H \\ G \end{pmatrix} \\
&= \left(H^T\mathbf{a}^1 + G^T\mathbf{v}^1\right) H + \left(H^T\mathbf{h}^1 + G^T\mathbf{d}^1\right) G \\
&= H^T\mathbf{a}^1 H + G^T\mathbf{v}^1 H + H^T\mathbf{h}^1 G + G^T\mathbf{d}^1 G.
\end{aligned}$$

This results in a convenient formula for reconstructing a signal from its decomposed form, that is,

$$\mathbf{f} = H^T\mathbf{a}^1 H + H^T\mathbf{h}^1 G + G^T\mathbf{v}^1 H + G^T\mathbf{d}^1 G. \tag{14}$$

3.6 Image Decomposition

In more practical applications, we decompose larger color image matrices. One of the test images used in this project, Lena, is represented as three 512×512 matrices, one for each color channel. The original image is decomposed into the first-level details, represented in grayscale as an image box. Figure 2 shows the original Lena image (a) and the first three decompositions (b), (c), and (d).

The multi-level decompositions are obtained iteratively by decomposing the average detail submatrix while the previous difference details are retained. Since the image matrices are finite, there is a limit to how many decompositions can be performed. For example, when the Lena image is decomposed once, the image approximation (average detail) becomes half the size, 256×256. Continuing this, the image approximation becomes "worse" as the number of levels increase. By the ninth decomposition, the average detail is reduced to a single pixel and no more decompositions are possible. At this point, the decomposition matrix is almost entirely made up of difference details. Natural images, those composed of people and objects and scenes, contain separate regions of similar hues and luminosity. Hence, the difference details will have smaller values inside these regions and larger values at the boundaries.

(a) Original Lena image.

(b) First-level image decomposition.

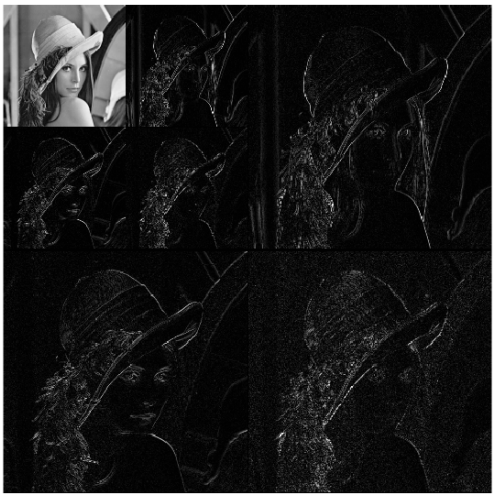

(c) Second-level image decomposition.

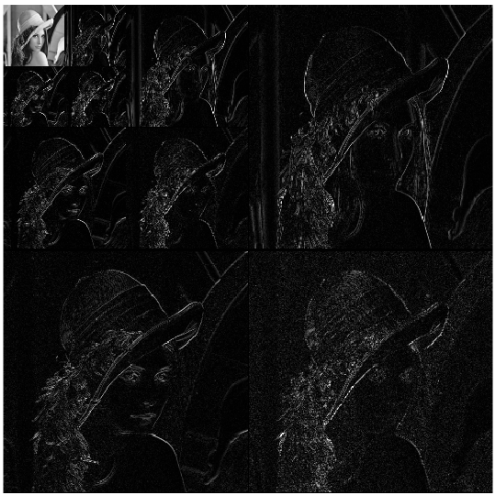

(d) Third-level image decomposition.

Figure 2: Multi-level two-dimensional Haar wavelet image decomposition.

4 Image Compression

When applying multi-level decompositions, the amount of data being stored in the decomposed matrix is the same as the original matrix. Since no information has been lost, the signal can always be perfectly reconstructed. This also means that the file size stored in memory has not been reduced.

4.1 Thresholding

In the previous section, we discussed how decomposing an image can result in small difference details. If the magnitudes of the differences are small enough, say less than some λ, then we can replace the difference value with a zero. This is known as thresholding, which handles the actual compression. A larger threshold number for λ gives better compression, however, if λ is too large, then much of the image quality will be lost.

We represent thresholding by the transform

$$T(x;\lambda) = \begin{cases} 0, & |x| \leq \lambda, \\ x, & |x| > \lambda, \end{cases} \tag{15}$$

where x is an element of the k-level wavelet decomposition of a signal $\mathbf{f}$. Since T maps multiple values between $-\lambda$ and λ to zero, the transformation is not one-to-one. Thus, T is not invertible, so the original image cannot be perfectly reconstructed. However, the thresholded matrix is more sparse, which results in reduced file size as desired.

In particular, Equation (15) is known as hard thresholding. Other types of thresholding (e.g. soft) are common and use neighboring pixels to blend the image. This leads to a variety of wavelet applications in denoising images and data.

4.2 Method

In MATLAB, we can import a color image as a 3-dimensional array with the command `imread('filename.png')` in RGB or YCbCr color space[3].

Using the Wavelet Toolbox, we perform the two-dimensional decomposition of each image layer with `wavedec2(x,k,wname)`. This function requires three parameters: a 2-dimensional array representing the image color

[3]For wavelet decomposition, YCbCr is preferred since RGB layers are usually correlated. So, an image is converted using `rgb2ycbcr(image)`.

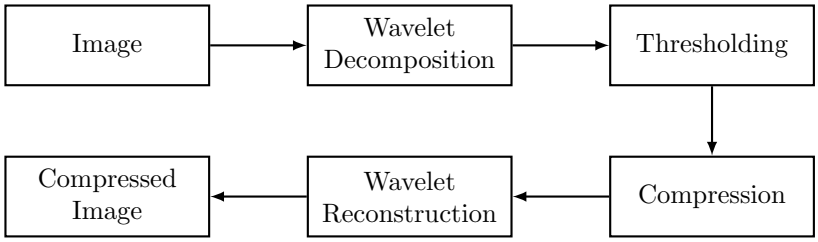

Figure 3: Wavelet image compression process diagram.

layer, an integer representing the number of levels of decomposition, and a string representing the name of the wavelet. For our purposes, we will use `'haar'` for the wavelet name and the maximum level of decompositions, `k` = floor($\log_2(\min\{m, n\})$), where the image dimensions are m pixels by n pixels. The outputs for each layer will be a decomposition vector `C` and a coefficient matrix `S`.

Compression is handled by `wdencmp('gbl',C,S,wname,k,thr,sorh,1)`. Parameters `C` and `S` are passed in from the `wavedec2` outputs, `wname` and `k` are reused, `thr` is the thresholding value, and `sorh` is either `'s'` (for soft thresholding) or `'h'` (for hard thresholding).

Lastly, the image is reconstructed by creating a 3-dimensional array from the outputs of `wdencmp()` performed on each color layer. This process is summarized in Figure 3.

4.3 Performance

The compression ratio (CR) is computed by comparing the original image file size to the compressed image file size. Using various threshold values λ, we compress standard test images, Lena and Peppers, with the Haar wavelet in MATLAB with hard thresholding in YCbCr color space. The results are in Table 1 and corresponding Figures 4 and 5.

Notice that as the threshold value increases, especially at $\lambda = 20$, the quality of the image degrades. As well, box-shaped artifacts become more noticeable making the image appear pixelated. This is actually due to the shape of the Haar wavelet being embedded when the difference details are thresholded. Further, we see in Table 1 that the compression ratio increases with larger threshold values. This indicates a tradeoff between compression and quality.

Image	λ	Orig. Size	Comp. Size	CR
Lena	5	465.09 KB	272.53 KB	1.7
$\cdots$	10	$\cdots$	150.63 KB	3.1
$\cdots$	20	$\cdots$	86.794 KB	5.4
Peppers	5	280.85 KB	122.40 KB	2.3
$\cdots$	10	$\cdots$	81.078 KB	3.5
$\cdots$	20	$\cdots$	51.649 KB	5.4

Table 1: Compression ratio for test images.

Ultimately the threshold value should be chosen to suit the needs of the application. One could proceed by comparing other wavelets and threshold values to achieve improved results.

5 Conclusion

We can outline the study of wavelets in a variety of ways. Wavelet bases can be viewed as a generalization of the basis functions in Fourier series. Using Multiresolution Analysis, we can describe wavelet decompositions as paired sequences of approximations and errors. In applications such as image compression, noise reduction, and signal smoothing, wavelets can be experienced hands-on using computational tools such as MATLAB. Although there are many more families of wavelets, the Haar wavelet provides a unique and friendly approach to understanding wavelets.

(a) Original (465.09 KB)

(b) Compressed $\lambda = 5$ (272.53 KB)

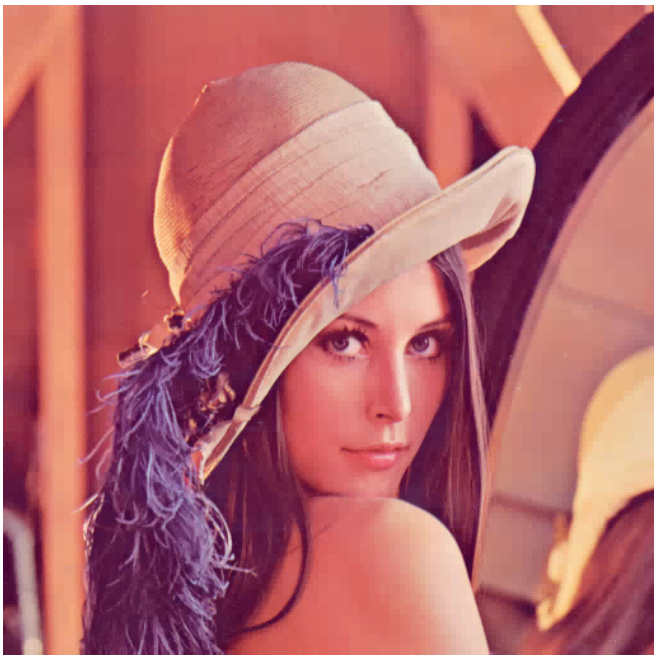

(c) Compressed $\lambda = 10$ (150.63 KB)

(d) Compressed $\lambda = 20$ (86.794 KB)

Figure 4: Lena image comparison.

(a) Original (280.85 KB)

(b) Compressed $\lambda = 5$ (122.40 KB)

(c) Compressed $\lambda = 10$ (81.078 KB)

(d) Compressed $\lambda = 20$ (51.649 KB)

Figure 5: Peppers image comparison with details.

References

[1] Edward Aboufadel and Steven Schlicker. *Discovering Wavelets*. John Wiley & Sons, 1999.

[2] Ingrid Daubechies. *Ten Lectures on Wavelets*. SIAM, 1992.

[3] Stéphane Mallat. *A Wavelet Tour of Signal Processing: The Sparse Way*. Academic Press, Inc., 3rd edition, 2008.

[4] Richard E. Woods Rafael C. Gonzalez and Steven L. Eddins. *Digital Image Processing Using MATLAB*. McGraw Hill, 2nd edition, 2011.